CIT04-0498

A COMPARISON BETWEEN FINITE VOLUME AND FINITE ELEMENT METHODS FOR TIME DEPENDENT CONDUCTION PROBLEMS

Nancy Mieko Abe[*]
Francisco D. Rocamora Jr.[**]
Angelo Passaro[*]
*EFA,**ENU-T
Instituto de Estudos Avançados - IEAv/CTA
Rod. dos Tamoios, Km 5,5, 12231-970 - São José dos Campos - SP, Brazil
rocamora@mec.ita.br

Abstract. In this work a comparison is made between the finite volume and the finite element methods regarding to the solution of 2D transient conduction problems subjected to several types of boundary conditions. The first problem examined is the semi-infinite medium with heat flux condition on the free surface. This problem is of particular interest for thermal shields based on the ablation phenomenon. Also, the problem of a slab with convection BC's on both surfaces is examined in order to compare the performance of both methods subjected to different BC's. A totally implicit scheme is used for the time dependent problem for both methods.

***Keywords**. Transient Heat Transfer, Numerical Methods,*

1. Introduction

A variety of problems occurring in engineering and sciences involve transient behavior in heat transport. In particular, in accident analysis it is often very important to be able to predict accurately transient temperature fields in devices, equipments, or even systems, in order to make sure the temperature and heat flux limits will not be surpassed. Also, in some processes the rate of heating or cooling has to be kept within pre-established limits. In this work, transient conduction problems with different types of boundary conditions are solved using two methods, finite volume and finite element schemes, in order to assess their accuracy. This work is inserted in a software platform development project for the analysis and design of devices, considering several physical phenomena such as electromagnetic wave propagation, plasma physics, and heat and mass transport (Abe *et al*. (2002), Franco *et al*. (1998), Franco *et al*. (1999)), and is part of an effort to validate mathematical and numerical formulations and the corresponding computational implementation. First, a semi-infinite medium subjected to a uniform heat flux condition on the free surface is analyzed. Then, a slab with internal heat generation and convection BC's on both surfaces is solved. The first case is of interest in thermal shield problems based on the ablation phenomenon, while the second can simulate the behavior of a nuclear fuel element under accident conditions in which there is a core flooding, for example.

2. Geometry of the Problems

For the case of the semi-infinite medium, the geometry considered was a horizontal slab insulated on three sides and with an imposed uniform heat flux on the other, as shown in Fig. (1).

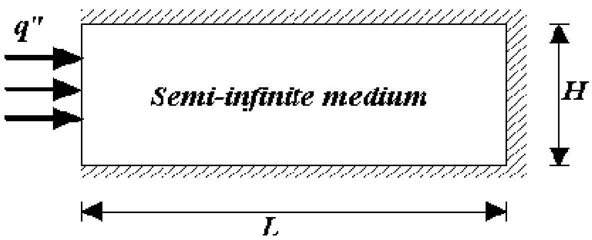

Figure 1 - Semi-Infinite Medium

The length of the slab, L , is made as big as necessary such that the side opposed to the heat flux has no or little influence on the behavior of the thermal field. This length depends on the time span one wishes to analyze. The height, H , on the other hand, is not important at all, since the applicable boundary conditions on both top and bottom sides are symmetry conditions. An analytical solution for this problem can be obtained from Holman (1976).

For the case of the heat generating vertical slab with convection BC's on both sides, a sketch of the geometry considered is shown in Fig. (2) below. Notice that, in this case, a heat transfer coefficient, h , has to be supplied.

These two geometries are then used to compare transient results between the finite volume and finite element schemes. It should be pointed out that, although the programs used are both for 2D geometries, the imposed boundary conditions for the two geometries reduce the problems to 1D.

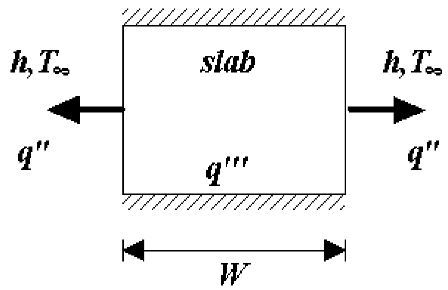

Figure 2 - Heat Generating Vertical Slab

3. Mathematical and Numerical Modeling

Here the two methods, finite volume and finite element, are presented and discussed briefly. For the two cases presented, the mathematical model is the time dependent energy equation with constant properties for the materials. This equation can be written as:

$$\rho c_p \frac{\partial T}{\partial t} = k\nabla^2 T + q''' \tag{1}$$

The boundary conditions applicable can be written as:

$$k\left.\frac{\partial T}{\partial n}\right|_{s-} = q_s'' \quad \text{for uniform heat flux BC,} \tag{2}$$

$$k\left.\frac{\partial T}{\partial n}\right|_{s-} = h\left(T_s - T_\infty\right) \quad \text{for the convection BC, and} \tag{3}$$

$$k\left.\frac{\partial T}{\partial n}\right|_{s-} = 0 \quad \text{for symmetry BC.} \tag{4}$$

In Eqs. (2) to (4) s^- represents approaching the boundary from the interior and n the normal direction to the boundary pointing outwards. Here, ρ is the material density, c_p is the specific heat, k is the thermal conductivity, q''' is the volumetric heat generation rate, q_s'' is the heat flux on a surface, T_s is the surface temperature and T_∞ is the ambient temperature.

3.1.The finite volume method

The finite volume method is based on the volume integral of the conservation equations over a control volume (CV, the cells of the discretized domain). The values of the quantities on the control volume's borders necessary to carry out this integration are obtained through some interpolation scheme. This procedure yields a set of algebraic equations for the variable of interest, which can be solved directly or by some sort of iterative procedure. Figure (3) shows a typical CV used in the discretization process. The CV shown is for a non-orthogonal structured mesh, although the meshes used in the solution of the proposed problems are orthogonal structured ones. Integrating Eq. (1) over this control volume one obtains:

$$\int_{\delta V}\left(\rho c_p \frac{\partial T}{\partial t}\right)dV = \int_{\delta V}\left(k\nabla^2 T\right)dV + \int_{\delta V} q''' dV \tag{5}$$

which can also be written as:

$$\int_{\delta V}\left(\rho c_p \frac{\partial T}{\partial t}\right)dV = \int_{\Gamma}\left(k\nabla T\right)dS + \int_{\delta V} q''' dV \tag{6}$$

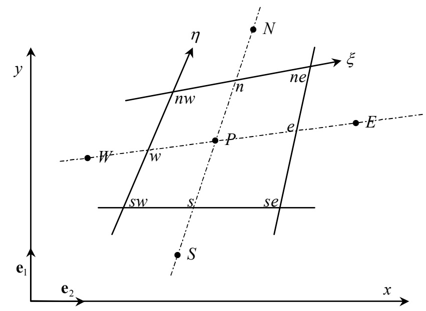

Figure 3 - Control Volume

where Γ is the CV boundary.

The left hand side and the second term on the right hand side of Eq. (6) are calculated using the variable values at the center of the control volume. The first term on the right hand side gives the heat fluxes at the CV faces.

The algebraic equation obtained with the application of the finite volume method to a CV has the following form:

$$I_e + I_w + I_n + I_s = S_\varphi \tag{7}$$

where φ is the variable of interest, I represent the fluxes of φ through the CV faces (east, west, north and south) and S is the source term inside the CV. The interpolation scheme used in this work is the central differencing scheme (CDS), which is linear. In the numerical procedure the system of equations obtained applying Eq. (7) to all the CV's in the domain is solved until the sum of the residues, *i.e.*, the difference between the right hand side and left hand side of Eq. (7), reaches a value lower than 10^{-5}, so the solution is considered converged. The time scheme utilized is the totally implicit scheme.

3.2. The finite element method

The finite element method (FEM) is based on the minimization of a functional whose solution is equivalent to the original differential equation. An approximated solution T for the differential equation (1) can be obtained by applying the Weighted Residual Method (WRM) or by applying variational principles. In the WRM, the integral of the residues, I, over the entire domain Ω is imposed equal to zero:

$$I = \int_\Omega W_0\, R_0\, d\,\Omega + \int_{\Gamma_1} W_1 R_1\, d\Gamma + \int_{\Gamma_2} W_2 R_2\, d\Gamma = 0 \tag{8}$$

where

$$R_0 = k\nabla^2 T - \rho\, c_p \frac{\partial T}{\partial t} + q''' \tag{9}$$

$$R_1 = T_s - T_\infty \tag{10}$$

$$R_2 = g_n - g \tag{11}$$

The time independent weighting functions, W_0, W_1 and W_2, are chosen arbitrarily, but they must be sufficiently regular in order to obtain finite integrals. The residue is minimized in a global sense.

The domain Ω is discretized in sub-domains of simple geometry named finite elements and Eq. (8) is supposed to be valid for each element. After some algebraic manipulation, the residue equation for each element can be written as follows:

$$\int_{\Omega^\xi} \nabla W_0^{(\xi)} \cdot (k\nabla T^{(\xi)}) d\Omega + \int_{\Omega^\xi} W_0^{(\xi)} \rho\, c_p \frac{\partial T^{(\xi)}}{\partial t} d\Omega - \int_{\Omega^\xi} W_0^{(\xi)} q'''^{(\xi)}\, d\Omega - \int_{\Gamma_2^\xi} W_0^{(\xi)} g^{(\xi)}\, d\Gamma = 0 \tag{12}$$

Inside each element, ξ, the state variable is expanded by using a finite set of linearly independent base functions $N_i^{(\xi)}$:

$$T^{(\xi)}(\vec{r}_j) = \sum_{i=1}^{n_0} N_i^{(\xi)}(\vec{r}_j)\, T_i^{(\xi)}, \qquad (13)$$

where $T_i^{(\xi)}$ is the temperature computed in the nodal point i and n_0 is the number of nodal points of the element.

These base functions depend on both the family and the approximation order of the finite elements adopted. The base functions present the following property:

$$N_i^{(\xi)}(\vec{r}_j) = \delta_{ij}\,, \qquad (14)$$

and obey the unit partition condition:

$$\sum_{i=1}^{n0} N_i^{(\xi)} = 1 \qquad (15)$$

In order to solve Eq. (12), the weighting functions are chosen by using the Galerkin technique, *i.e.*, the weighting functions coincide with the base functions:

$$W_{0_i}^{(\xi)} = N_i^{(\xi)}\,. \qquad (16)$$

The final equation for each element expressed in a matrix form is:

$$\left([\, S \,] + [\, D \,] \right) \{\, T \,\}^T + [\, C \,] \left\{ \frac{\partial T}{\partial t} \right\}^T = \{\, P \,\}^T + \{\, G \,\}^T \qquad (17)$$

where the elements of the matrices are:

$$S_{ij}^e = \int_{\Omega^e} \nabla N_j \cdot (k \nabla N_i)\, T_i \, d\Omega \qquad (18)$$

$$D_{ij}^e = \int_{\Gamma_2^e} N_j N_i \, h_c \, T_i \, d\Gamma \qquad (19)$$

$$C_{ij}^e = \int_{\Omega^e} N_j \, N_i \, \rho \, c_p \, d\Omega \qquad (20)$$

$$P_{ij}^e = \int_{\Omega^e} N_j \, q''' \, d\Omega \qquad (21)$$

$$G_{ij}^e = \int_{\Gamma_2^e} N_j \, q_s'' \, d\Gamma + \int_{\Gamma_2^e} N_j \, h_c \, T_c \; d\Gamma \qquad (22)$$

The index ξ in the integrals was omitted.

3.3. Time discretization scheme

The time discretization is accomplished by the following scheme (Zienkiewics and Taylor (1991)):

$$T_{n+1} = T_n + \Delta t \left[(1-\Theta) \frac{\partial T_n}{\partial t} + \Theta \frac{\partial T_{n+1}}{\partial t} \right], \qquad 0 \le \Theta \le 1 \qquad (23)$$

where Θ is an adimensional value. By selecting specific values for Θ it is possible to recover several different time schemes, from the Euler explicit method (Θ=0) to a totally implicit one (Θ=1). Substituting the first derivative in time of T_n in Eq. (17) results the formulation used in this work:

$$\left(\Theta(S+D) + \frac{C}{\Delta t} \right) T(t+\Delta t) = \left(-(1-\Theta)\,(S+D) + \frac{C}{\Delta t} \right) T(t) \; + \\ \big((1-\Theta) P(t) \; + \Theta P(t+\Delta t) \big) + \big(\, (1-\Theta)\, G(t) + \Theta G(t+\Delta t) \big) \qquad (24)$$

4. Results and Discussion

In this work two time dependent problems were solved, using both methods described in the previous section, in order to compare them. For both methods care was taken so that the number of 'volumes' obtained in the meshing process was about the same. The results obtained are summarized below.

4.1. Semi-Infinite Medium

For the semi-infinite medium subjected to a uniform heat flux at the free surface, the results of the two methods are compared to the analytical solution at several time instants. The medium properties as well as the initial and boundary conditions utilized are shown in Tab (1). Tables (2), (3) and (4) summarize the results obtained for the surface temperature and for 2.5 cm and 10 cm deep temperatures, together with the relative errors with respect to the analytical solution.

Table 1 - Semi-infinite medium properties and BC's.

Physical Model	
Material:	Thermal conductivity k = 45 W/(m °C). Thermal diffusivity α = 1.4 10^{-5} m^2/s
Initial condition:	uniform temperature T_i = 35°C
Boundary Condition:	imposed uniform heat flux q'' = 3.2 x10^5 W/m^2

Table 2 - Surface temperature for several time instants for the Semi-infinite medium and associated errors.

t (s)	Analytical solution	FEM L = 10 cm	FEM L = 50 cm	FVM L = 50cm	error(%) FEM L = 10 cm	error(%) FEM L = 50 cm	error(%) FVM L = 50 cm
15	151.279	150.263	150.265	154.22	0.671611	0.6702897	1.944086
30	199.4	198.723	198.725	201.53	0.3395119	0.3385094	1.068207
45	236.4	235.813	235.815	238.11	0.2483039	0.2474583	0.7233531
60	267.547	267.049	267.05	269.05	0.1861302	0.1857652	0.561767
75	295	294.555	294.55	296.34	0.1508499	0.1525465	0.4542361
100	335.23	334.872	334.838	336.39	0.1067929	0.1169341	0.3460322
200	459.59	461.864	459.313	460.42	0.4947926	6.027286E-2	0.1805995
300	555.02	568.331	554.789	555.7	2.398287	4.162338E-2	0.1225168
400	635.46	669.638	635.266	636.06	5.378462	3.053391E-2	9.441595E-2
500	706.33	769.637	706.162	706.88	8.962809	2.378913E-2	7.786556E-2

Table 3 - Temperature at 2.5 cm from the surface for several time instants for the Semi-infinite medium and associated errors.

t (s)	Analytical solution	FEM L = 10 cm	FEM L = 50 cm	FVM L = 50cm	error(%) FEM L = 10 cm	error(%) FEM L = 50 cm	error(%) FVM L = 50 cm
15	50.695	50.911	50.882	52.789	0.4260767	0.3688732	4.130589
30	79.3	79.204	79.1703	81.123	0.1210601	0.1635557	2.298862
45	106.606	106.4	106.37	108.18	0.1932361	0.2209975	1.476462
60	131.73	131.51	131.479	133.15	0.1670092	0.1905351	1.077961
75	154.099	154.757	154.715	156.27	0.4270013	0.3998705	1.408838
100	190.35	190.216	190.81	191.49	7.039805E-2	0.2416556	0.5988964
200	305.22	309.049	305.06	306.12	1.254508	0.0524224	0.2948673
300	396.46	413.49	396.267	397.17	4.295515	0.0486791	0.1790904
400	474.36	514.283	474.185	474.98	8.416189	3.688924E-2	0.1307078
500	543.45	614.152	543.33	544.44	13.00984	2.208025E-2	7.786556E-2

Table 4 - Temperature at 10,0 cm from the surface for several time instants for the Semi-infinite medium and associated errors.

t (s)	Analytical solution	FEM L = 10 cm	FEM L = 50 cm	FVM L = 50cm	error(%) FEM L = 10 cm	error(%) FEM L = 50 cm	error(%) FVM L = 50 cm
15	34.997	35.0008	35.004	35.001	1.085647E-2	2.000163E-2	1.142327E-2
30	35.028	35.0974	35.0491	35.062	0.1981295	6.023493E-2	9.706634E-2
45	35.36	35.861	35.4319	35.487	1.416854	0.2033354	0.3591598
60	36.403	38.035	36.5202	36.637	4.483147	0.3219486	0.6428074
75	38.35	41.974	38.4909	38.674	9.449806	0.3674046	0.8448535
100	43.54	52.3739	43.6926	43.794	20.28916	0.3504808	0.5833666
200	79.83	124.821	79.9111	80.397	56.35851	0.1015915	0.710261
300	125.99	217.467	126.05	126.6	72.60655	4.762695E-2	0.4841659
400	173.72	315.271	174.104	174.67	81.48227	0.2210469	0.5468553
500	221.68	414.383	221.642	222.93	86.92846	1.713929E-2	0.5638759

The Tables illustrate the effect of the domain truncation (L length) on the results for the FE computation. The same effect is obtained for the FVM. For a compatible choice of the domain truncation, both methods present adequate precision from an engineering point of view. The presented results were obtained for a time step equal to 1 s. As can be also noticed from the Tables, the FVM consistently overestimates the analytical results for the set of numerical parameters used, such as time step, number of volumes and tolerance.

Fig. (4) illustrates the temperature profile obtained from the analytical solution and the numerical methods for several time instants. In both cases, the length L is 50 cm.

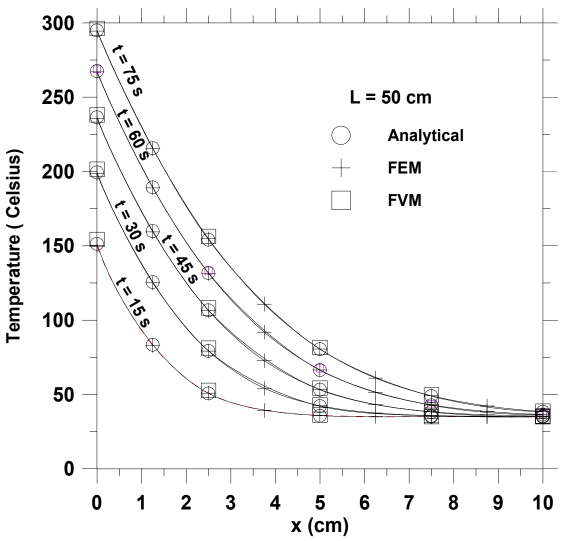

a)

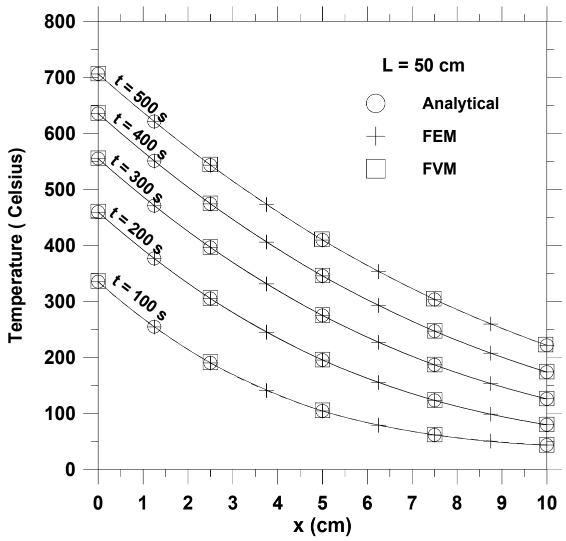

b)

Figure 4 - Temperature profile as a function of x for different time instants: (a) from 15 to 75 s and (b) from 100 to 500 s.

As can be noticed, for a time instant up to about 60 s, the temperature at a depth of 10 cm does not change much, which justify the results obtained for L =10 cm being reasonable up to about 100 s. After that, though, the influence of the length L on the results is evident.

4.2.Infinite Heat Generating Slab

For the case of the heat generating vertical slab with convection BC's on both sides, the results of the two methods are compared to each other at several time instants. The material properties as well as the initial and boundary conditions utilized are shown in Tab. (5). Tables (6) and (7) summarize the results obtained at t = 200 s and t = 1000 s for two different time steps.

Table 5 - Material properties and boundary conditions.

Geometry	Slab width $W = 5$ cm.
Material:	Thermal conductivity $k = 1$ W/(m °C). Density $\rho = 100$ kg/m^3 Specific heat: $c_p = 3600$ J/kg °C
Source:	$q''' = 1\text{x}10^5$ W/m^3
Initial condition:	uniform temperature $T_i = 20$°C
Boundary Condition:	Convective surfaces: $h = 100$ W/m^2 °C e $T_\infty = 20$ °C.

Table 6 - Computed temperatures for t = 200s.

	$\Delta t = 5\ s$			$\Delta t = 1\ s$		
x(m)	FEM	FVM	Difference (%)	FEM	FVM	Difference (%)
0	37.4128	37.81691	1.080138	37.5121	37.65425	0.3789467
0.005	45.0833	45.53851	1.009704	45.2291	45.30149	0.1600552
0.01	50.8406	51.34755	0.9971369	51.0253	51.0481	4.468459E-2
0.015	54.8417	55.38994	0.9996715	55.0558	55.04336	2.259476E-2
0.02	57.1923	57.77633	1.021169	57.4246	57.40042	4.210313E-2
0.025	57.9742	58.575	1.036322	58.2128	58.189	4.08843E-2
0.03	57.1951	57.80934	1.073943	57.4275	57.43301	9.591959E-3
0.035	54.8427	55.45694	1.120001	55.0568	55.10954	9.578869E-2
0.04	50.8397	51.45046	1.201344	51.0244	51.14983	0.2458256
0.045	45.0827	45.68011	1.325147	45.2285	45.44164	0.4712484
0.05	37.4128	38.00062	1.571179	37.5121	37.83631	0.8642841

Table 7 - Computed temperatures for t = 1000 s.

	$\Delta t = 5\ s$			$\Delta t = 1\ s$		
x(m)	FEM	FVM	Difference (%)	FEM	FVM	Difference (%)
0	44.9219	45.17406	0.5613278	44.9269	45.18114	0.5659014
0.005	56.1147	56.2712	0.2788894	56.122	56.28226	0.2855551
0.01	64.8202	64.90586	0.1321546	64.8295	64.91988	0.1394202
0.015	71.0454	71.07997	4.865732E-2	71.0562	71.09598	5.598338E-2
0.02	74.7779	74.79452	2.222157E-2	74.7896	74.81152	2.931809E-2
0.025	76.0321	76.05	2.355083E-2	76.044	76.067	3.02491E-2
0.03	74.7814	74.84641	8.693347E-2	74.7931	74.86341	9.400934E-2
0.035	71.0461	71.18375	0.1937468	71.0568	71.1998	0.2012443
0.04	64.8193	65.06155	0.373729	64.8286	65.07561	0.381019
0.045	56.114	56.47882	0.6501451	56.1213	56.48996	0.6568985
0.05	44.9219	45.43367	1.13924	44.9269	45.44083	1.143928

In Tables (6) and (7) the percent difference between the two methods is calculated based on the FEM results.

Figure (5) shows the temperature profiles obtained by the two methods using time steps of 5 s and 1 s. It is expected that a smaller time step yield more accurate results. The biggest differences occur in the beginning of the simulation, which is illustrated at the time instant = 200 s. In this case, a more detailed analysis shows that when the time step is reduced from 5 to 1 s the results obtained by FVM decrease while the ones obtained by FEM increase, *i.e.*, the methods tend to converge as shown in Fig. (6). It should also be observed that, for this problem a steady state is reached after enough time is elapsed, so that the differences between the methods will be due to the spatial discretization only.

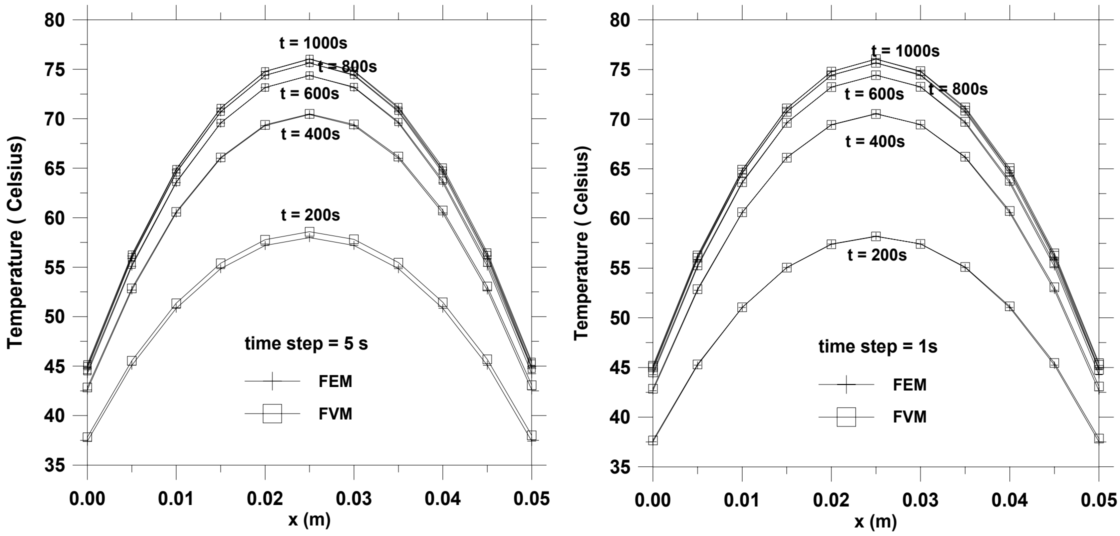

a) b)

Figure 5 - Temperature profile as a function of x for several time instants: (a) for time step equal to 5 s and (b) for time step equal to 1 s.

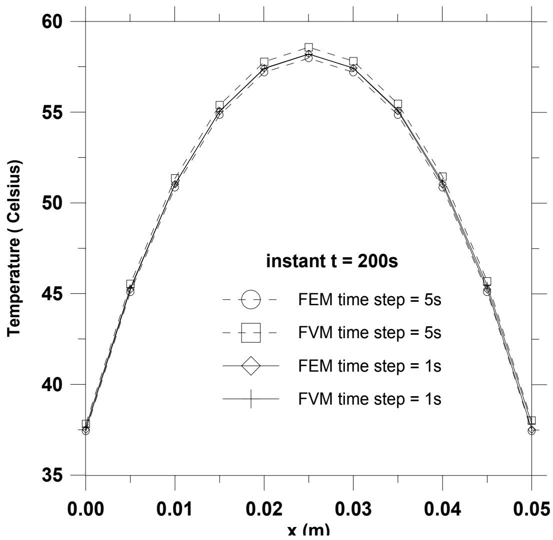

Figure 6 - The temperature profile at 200 s obtained by the two methods for time steps of 5 and 1 s.

5.Conclusion

The results obtained by applying both the FEM and the FVM to two simple, one-dimensional, transient conduction problems are presented in this work. The problems were chosen in order to evaluate several details of the methods' implementation such as the treatment of different boundary conditions and volumetric heat sources. The comparisons made between the methods showed that, for the type of transients analyzed and the choices of parameters for both methods, *i.e.*, base functions, interpolation functions, etc., both yield accurate results with a totally implicit time scheme. As expected, for smaller time steps the methods get closer to one another. For the semi-infinite medium problem, which is also compared to an analytical solution, the FEM showed slightly better results than the FVM.

The generated documentation serves as a tutorial for potential users of the software platform under development and gives us confidence to continue the implementation of software modules for the study of additional phenomena, such as the analysis of convective heat transfer for turbulent incompressible flow.

6. Acknowledgement

This work is supported by FAPESP under Process. n. 03/06888-1.

7. References

Abe, N. M., Passaro, A., Franco, M. A.R., Sircilli, F., Serrão, V. A., Odan, D. H. and Santos, F. J. R., 2002, 'Um Sistema de Software para Análise de Dispositivos e Componentes de Óptica Integrada, Fibras Ópticas e Microondas', in *Anais do V Congresso Brasileiro de Eletromagnetismo* - CBMAG 2002, CD-ROM, 04 a 06 de Novembro, Gramado, RS.

Franco, M.A.R., Passaro, A., Sircilli, F. e Cardoso, J.R., 1998, 'Modal Analysis of Anisotropic Diffused-Channel Waveguide by a Scalar Finite Element Method', *IEEE Transactions on Magnetics*, vol.34, No. 5, pg. 2783-2786.

Franco, M.A.R., Passaro, A., Cardoso, J.R., Machado, J.M., 1999, 'Finite Element Analysis of Anisotropic Optical Waveguide with Arbitrary Index Profile', *IEEE Transactions on Magnetics*, vol. 35, No. 3, pg. 1546-1549.

Kreith, F., Black, W. Z., 1980, BASIC HEAT TRANSFER, Harper &Row, New York.

Lapidus, L, Pinder, G. F., 1982, NUMERICAL SOLUTION OF PARTIAL DIFFERENTIAL EQUATIONS IN SCIENCE AND ENGINEERING, John Wiley & Sons.

Maliska, C. R., 1995, TRANSFERÊNCIA DE CALOR E MECÂNICA DOS FLUIDOS COMPUTACIONAL, LTC.

Özişik, M. N., 1985, HEAT TRANSFER - A Basic Approach, Mc-Graw Hill.

Patankar, S.V., 1980, NUMERICAL HEAT TRANSFER AND FLUID FLOW, Mc-Graw Hill.

Rocamora, F.D. and de-Lemos, M.J.S., 2000, Analysis of Convective Heat Transfer for Turbulent Flow in Saturated Porous Media, *Int. Comm. Heat Mass Transfer*, vol. 27, n. [illegible]. 825-834.

J.P. Holman, 1976., HEAT TRANSFER, International Student Edition, McGraw-Hill Kogakusha, 4a. ed.

O. C. Zienkiewics and R. L. Taylor, , 1991. THE FINITE ELEMENT METHOD, McGraw-Hill Book Company, vol. 2, 4a. ed.

8. Copyright Notice